Uncovering a context-specific connectional fingerprint of human dorsal premotor cortex

Moisa, Marius ; Siebner, Hartwig R ; Pohmann, Rolf ; Thielscher, Axel

Abstract: Primate electrophysiological and lesion studies indicate a prominent role of the left dorsal premotor cortex (PMd) in action selection based on learned sensorimotor associations. Here we applied transcranial magnetic stimulation (TMS) to human left PMd at low or high intensity while right-handed individuals performed externally paced sequential key presses with their left hand. Movements were cued by abstract visual stimuli, and subjects either freely selected a key press or responded according to a prelearned visuomotor mapping rule. Continuous arterial spin labeling was interleaved with TMS to directly assess how stimulation of left PMd modulates task-related brain activity depending on the mode of movement selection. Relative to passive viewing, both tasks activated a frontoparietal motor network. Compared with low-intensity TMS, high-intensity TMS of left PMd was associated with an increase in activity in medial and right premotor areas without affecting task performance. Critically, this increase in task-related activity was only present when movement selection relied on arbitrary visuomotor associations but not during freely selected movements. Psychophysiological interaction analysis revealed a context-specific increase in functional coupling between the stimulated left PMd and remote right-hemispheric and mesial motor regions that was only present during arbitrary visuomotor mapping. Our TMS perturbation approach yielded causal evidence that the left PMd is implicated in mapping external cues onto the appropriate movement in humans. Furthermore, the data suggest that the left PMd may transiently form a functional network together with right-hemispheric and mesial motor regions to sustain visuomotor mapping performed with the left nondominant hand.

DOI: https://doi.org/10.1523/JNEUROSCI.2757-11.2012

Behavioral/Systems/Cognitive

Uncovering a Context-Specific Connectional Fingerprint of Human Dorsal Premotor Cortex

Marius Moisa,[1] Hartwig R. Siebner,[2] Rolf Pohmann,[1] and Axel Thielscher[1]

[1]High-Field Magnetic Resonance Center, Max Planck Institute for Biological Cybernetics, D-72076 Tübingen, Germany, and [2]Danish Research Centre for Magnetic Resonance, Copenhagen University Hospital Hvidovre, DK-2650 Hvidovre, Denmark

Primate electrophysiological and lesion studies indicate a prominent role of the left dorsal premotor cortex (PMd) in action selection based on learned sensorimotor associations. Here we applied transcranial magnetic stimulation (TMS) to human left PMd at low or high intensity while right-handed individuals performed externally paced sequential key presses with their left hand. Movements were cued by abstract visual stimuli, and subjects either freely selected a key press or responded according to a prelearned visuomotor mapping rule. Continuous arterial spin labeling was interleaved with TMS to directly assess how stimulation of left PMd modulates task-related brain activity depending on the mode of movement selection. Relative to passive viewing, both tasks activated a frontoparietal motor network. Compared with low-intensity TMS, high-intensity TMS of left PMd was associated with an increase in activity in medial and right premotor areas without affecting task performance. Critically, this increase in task-related activity was only present when movement selection relied on arbitrary visuomotor associations but not during freely selected movements. Psychophysiological interaction analysis revealed a context-specific increase in functional coupling between the stimulated left PMd and remote right-hemispheric and mesial motor regions that was only present during arbitrary visuomotor mapping. Our TMS perturbation approach yielded causal evidence that the left PMd is implicated in mapping external cues onto the appropriate movement in humans. Furthermore, the data suggest that the left PMd may transiently form a functional network together with right-hemispheric and mesial motor regions to sustain visuomotor mapping performed with the left nondominant hand.

Introduction

Functional neuroimaging studies in humans consistently indicate that the rostral part of the dorsal premotor cortex (PMd) is activated during movement selection (Picard and Strick, 2001). Recording of neuronal activity in primates during motor tasks suggest that the PMd preferentially maps external cues onto appropriate motor responses, whereas the medial areas are more involved in internally generated movements (Mushiake et al., 1991; Passingham et al., 2004). However, neuroimaging in humans failed to confirm such dissociation, showing similar activity increases in medial and lateral premotor areas, including the PMd, for internally triggered versus externally cued movements (Deiber et al., 1991; Jenkins et al., 2000; Weeks et al., 2001). Learning arbitrary visuomotor associations resulted in performance-dependent activity changes in medial areas but not PMd (Sakai et al., 1999; Toni et al., 2001; Eliassen et al., 2003; Bédard and Sanes, 2009). Finally, studies focusing on subprocesses of motor control, such as movement preparation or execution, reported similar activation time courses in medial areas and PMd (Richter et al., 1997; Cavina-Pratesi et al., 2006; Jankowski et al., 2009).

Inferences based on functional neuroimaging are correlative and, thus, cannot prove a causal involvement of PMd in conditional movement selection. Here, the combination of transcranial magnetic stimulation (TMS) with functional neuroimaging adds a causal dimension by transiently disrupting processing in left PMd while subjects perform a task (Siebner et al., 2009). If the PMd is functionally relevant to movement selection based on sensorimotor associations, TMS during a conditional sensorimotor task may trigger acute shifts in the weighted task-related activity in remote medial and lateral premotor areas. These activity changes can be mapped with functional magnetic resonance imaging (fMRI). Using an online TMS–fMRI approach, Bestmann et al. (2008) demonstrated state-dependent activity changes in right PMd during short high-frequency TMS bursts applied to left PMd: TMS of left PMd increased regional activity in right PMd and primary motor cortex when subjects performed a visually guided grip force task with their left hand. The same TMS had an opposite effect at rest, causing a decrease in activity in right PMd and primary motor area M1. These findings support the notion that the left PMd contributes to conditional visuomotor control, but the effects of TMS on task-related activity were demonstrated relative to passive viewing (PV) (Bestmann et al., 2008). Hence, it remained unclear whether the remote activations induced by TMS over left PMd were specifically related to sensorimotor mapping, other motor processes such as force generation, or simply caused by different levels of general motor activation.

Received May 31, 2011; revised Feb. 27, 2012; accepted April 3, 2012.

Author contributions: H.R.S. and A.T. designed research; M.M. performed research; R.P. contributed unpublished reagents/analytic tools; M.M. and A.T. analyzed data; M.M., H.R.S., and A.T. wrote the paper.

This work was supported by the Max Planck Society (M.M., R.P. and A.T.) and Grant of Excellence "ContAct" (Control of Actions) from the Lundbeckfonden (H.R.S.).

Correspondence should be addressed to Dr. Axel Thielscher, Max Planck Institute for Biological Cybernetics, Spemannstraße 41, D-72076 Tübingen, Germany. E-mail: axel.thielscher@tuebingen.mpg.de.

DOI:10.1523/JNEUROSCI.2757-11.2012

 0270-6474/12/327244-09$15.00/0

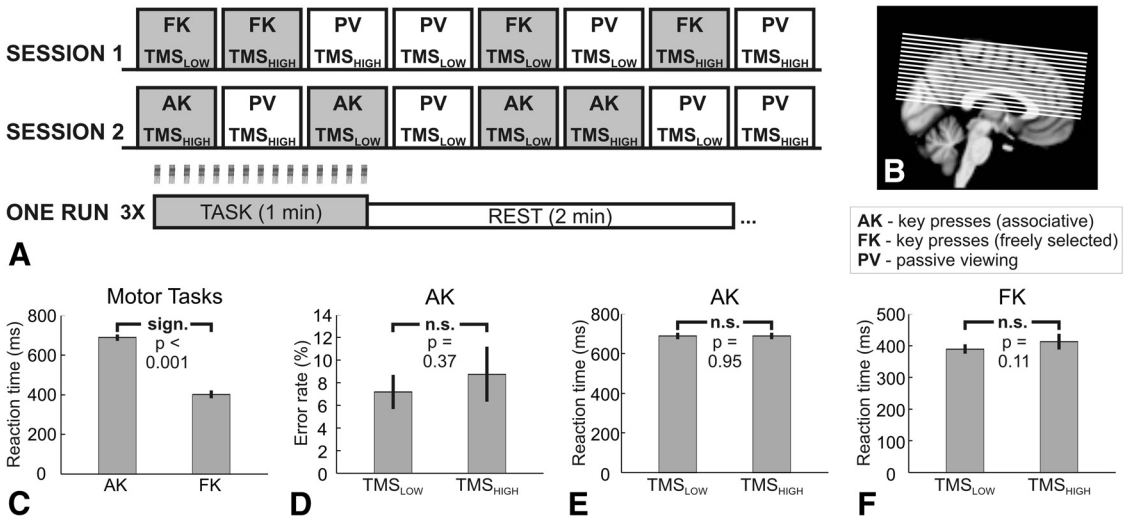

Figure 1. ***A***, Schematic diagram of the experimental design. One motor task was tested per session (either AKs or FKs), whereas PV was assessed in both sessions. One condition was investigated per experimental run. The order of runs within one session was pseudorandomized across subjects, and the order of sessions was counterbalanced across subjects. Each run consisted of three alternating epochs of task and rest, with task epochs lasting 60 s and rest epochs lasting 120 s. ***B***, Brain coverage of the CASL sequence. The field of view contained most of the cortical motor network. ***C***, RTs for the two different tasks, averaged across TMS intensities. ***D***, Error rates for the associative task in dependence on TMS intensity. ***E***, Dependence of RTs during the associative task on TMS intensity. ***F***, RTs during the free selection task in dependence on TMS intensity. In ***C–F***, the error bars represent the SE across subjects.

Here we interleaved TMS with continuous arterial spin labeling (CASL) (Moisa et al., 2010) to resolve this ambiguity. We compared the acute effects of TMS with left PMd on remote cortical activity during two high-level motor tasks that differed only in terms of movement selection. During online TMS–fMRI, right-handed subjects were asked to generate either externally or internally guided sequential key presses with their left nondominant hand. We hypothesized that a continuous train of TMS applied to left PMd would trigger context-specific activity shifts in remote premotor areas during externally but not internally guided movements.

Materials and Methods

Subjects. Nine right-handed volunteers with a mean age of 26 years (range, 24–31; five males and four females) participated in the study after they had given written informed consent. None of them had a history of neurological or psychiatric diseases or was on regular medication. The study was approved by the local ethics committee of the Medical Faculty of the University of Tübingen.

Experimental design. Figure 1*A* illustrates the experimental design. In a preparatory session, we acquired a high-resolution structural image and defined the site for TMS of the left PMd using neuronavigation. After the preparatory session, subjects participated in two experimental sessions in which we interleaved TMS and CASL-based fMRI while subjects performed externally paced sequential key presses with their left nondominant hand. In one experimental session, each finger movement was determined by an arbitrary nonspatial cue, here referred to as associative key presses (AKs). In the other experimental session, the cue only specified the timing of the movement, but subjects freely selected which finger to move, here referred to as freely selected key presses (FKs). Additional CASL fMRI runs in which participants only passively viewed the cues without performing any movement served as baseline condition. We did not alternate between the two motor tasks within one session to prevent putative crossover effects. In particular, we wanted to rule out any interfering effect of task switching on steady-state performance in the associative finger-tapping task. In addition, for those subjects who were tested on freely selected responses in the second session, the temporal separation rendered it unlikely that the results were biased by active suppression of the prelearned response mapping. The two experimental sessions were separated by at least 1 week, and the order of sessions was counterbalanced across subjects.

Here we assessed the regional cerebral blood flow (rCBF) based on CASL rather than measuring regional changes in the blood oxygen level-dependent (BOLD) signal as usually done in fMRI experiments. Our choice was motivated by three considerations. (1) We recently introduced the interleaved TMS–CASL method to capture acute effects of TMS on regional brain perfusion at rest (Moisa et al., 2010). In this study, we wanted to test whether CASL also has sufficient sensitivity to reveal acute TMS-induced changes in activation differences during motor tasks that only differ in terms of the mode of movement selection. (2) The good temporal stability of CASL–fMRI (Wang et al., 2003, 2005b) allowed us to test the effects of TMS on task-related perfusion changes separately in two experimental sessions that were well separated in time, minimizing any possible crossover effects (as outlined above). (3) The interleaved TMS–CASL method offered us the possibility to apply TMS bursts continuously during a 1 min period of sustained task performance (as indicated by Fig. 1*A*). We reasoned that the continuous perturbation during continuous task performance would be more suited to investigate the steady-state network activity subserving visuomotor mapping as opposed to a single TMS burst that is intermittently applied at low repetition rates in an event-related BOLD–fMRI design. It has been demonstrated that ASL can be advantageous compared with BOLD fMRI at these low task repetition frequencies (Aguirre et al., 2002; Wang et al., 2003).

Each TMS–CASL session consisted of eight runs. Four fMRI runs were acquired while subjects performed one of the two motor tasks (TASK), and four fMRI runs were obtained during PV (CONTROL). In two of the four TASK and CONTROL runs, we applied high-intensity or low-intensity TMS, respectively, with the order of experimental conditions being counterbalanced across subjects. Thus, the experiment had a two-factorial blocked design with the factor TMS intensity (two levels: TMS_{HIGH} vs TMS_{LOW}, within-session effect) and motor state (two levels: freely selected vs externally determined movements, between-session effect).

Experimental tasks. During task periods, subjects viewed a randomized sequence of five geometrical figures presented in the center of the visual field at a rate of 0.8 Hz. Subjects were required to produce a sequence of key presses with the fingers of their left hand in response to the visual cues. In experimental runs with AKs, each figure instructed a response with a specific finger. In experimental runs with FKs, subjects had to randomly select a new response each time a figure was displayed. Here the cues merely served to pace the movement but were not relevant in terms of which key to press. There were two restrictions to random

movement selection. Participants were not allowed to press the same key twice in a row to ensure a change in motor output from trial to trial. The subjects were also instructed not to perform an ascending or descending key-presses sequence. In the control runs, subjects had to passively view the figures without performing any movements.

Before CASL–fMRI, participants were trained on the tasks (AKs or FKs) that they were to perform in the MR scanner. In the training session, participants learned the specific associations between each geometrical figure and key press. Subjects practiced the task until they made no errors (3–10 min of practice) and were retested again immediately before the first fMRI run.

Using an epoch-related CASL–fMRI design, each run consisted of three alternating epochs of task and rest, with task epochs lasting 60 s and rest epochs lasting 120 s. During the rest periods, the subjects had to fixate a white cross presented in the central visual field. Visual stimulation and recording of the button presses was done using Cogent (Wellcome Department of Imaging Neuroscience, University College London, London, UK; http://www.vislab.ucl.ac.uk/cogent.php) programmed in MATLAB (MathWorks).

TMS. The site for TMS of the left PMd was identified in the TMS laboratory. We first defined the location of the primary motor hand area (M1-HAND). The M1-HAND site was functionally defined as the site on the skull where a clearly suprathreshold TMS pulse elicited the largest muscle twitch in the relaxed first dorsal interosseous muscle of the right hand. The M1-HAND site was then used as anchor point for defining the stimulation site in the left PMd. According to Schluter et al. (1998), the PMd site for TMS was located 2 cm anterior and 1 cm medial to the functionally defined M1-HAND site. The exact position of the TMS coil over the left PMd was saved using a neuronavigation system (BrainView; Fraunhofer IPA). This enabled us to precisely locate the PMd site with neuronavigated TMS in the following sessions of interleaved TMS–CASL imaging.

A MagPro X100 stimulator (MagVenture) with an MR-compatible figure-8 coil (MRi-B88) was used to deliver biphasic magnetic stimuli in the MR environment. The coil was positioned tangentially to the skull, with the induced current orientation being ~45° with the subject's body midline. Before each TMS–CASL session, the left M1-HAND and PMd sites were marked on the subject's skull based on the positions saved by the neuronavigation system. Inside the scanner, the TMS coil was first positioned over the M1-HAND using a custom-built MR-compatible coil holding device (Moisa et al., 2009), and individual resting (rMT) and active (aMT) motor thresholds were determined. After threshold measurements, the coil was positioned over the cortical target region, the left PMd.

During the TMS–CASL sessions, we delivered short high-frequency TMS bursts to the left PMd in the MR scanner while measuring changes in rCBF with interleaved CASL. TMS bursts were given at a high intensity (TMS_{HIGH} = 110% of individual rMT) or low intensity (TMS_{LOW} = 70% of individual aMT). High-intensity TMS was considered to be effective in modulating PMd activity. In contrast, low-intensity TMS was considered too weak to significantly modulate PMd activity but served as a high-level control for the nonspecific effects of TMS caused by acoustic and somatosensory stimulation. TMS consisted of high-frequency (10 Hz) bursts of five biphasic pulses with an interstimulus interval of 100 ms. TMS bursts were continuously applied during the task periods of the experimental runs with a 4.0 s gap between two consecutive bursts. The stimulus intensity was kept constant during a task block but pseudorandomized among the task blocks of an experimental run.

Interleaved TMS–CASL procedure. Scanning was performed on a 3 T Siemens TIM Trio. In the preparatory session, we acquired a high-resolution structural MRI of the whole brain (MPRAGE; 192 sagittal slices; matrix size, 256 × 256; voxel size, 1 mm^3; TR, 1900 ms; TE, 2.26 ms; TI, 900 ms, 12-channel head coil). During the experimental sessions, a one-channel radio frequency transmit/receive head coil (model PN 2414895; USA Instruments) was used for interleaved CASL–TMS.

An in-house-written CASL sequence with EPI readout (2D gradient-echo echo planar imaging) and separate radio frequency coils placed on the subject neck for labeling the inflowing blood in the right and left carotid was used for imaging (Zhang et al., 1995; Zaharchuk et al., 1999). Each of the eight experimental runs acquired per session contained 142 volumes (71 pairs of control–tag images; matrix size, 64 × 64; voxel size, 3 × 3 × 4 mm^3; 0.5 mm gap; TR, 4000 ms; TE, 20 ms; bandwidth, 2442 Hz/pixel; tag duration, 2343 ms; tag delay, 820 ms; tag gradient strength, 2.0 mT/m). One volume consisted of 16 slices covering the motor, premotor, frontal, and parietal areas (Fig. 1*B*). Before each functional scan, a control magnitude image was acquired (six volumes; TR, 8 s; no labeling and saturation pulses; all other parameters were identical to those of the functional images). The control magnitude images were used to check for systematic global differences in image intensities between sessions. Additionally, in the first session, a whole-brain EPI was acquired once that was used for image registration during post-processing (32 slices; matrix size, 64 × 64; voxel size, 3 × 3 × 4 mm^3; 0.5 mm gap; TR, 1600 ms; TE, 20 ms; bandwidth, 2442 Hz/pixel).

The 10 Hz repetitive TMS (rTMS) trains were applied during the tagging delay of the CASL sequence (starting directly after the end of tagging; stopping at least 100 ms before the EPI acquisition) to prevent any side effects of the TMS stimulation on the image acquisition (Bestmann et al., 2003; Moisa et al., 2010). Additional details on the interleaved TMS/CASL setup can be found in a study by Moisa et al. (2010).

Data analyses. Reaction times (RTs) were analyzed using a two-way repeated-measures ANOVA with TMS intensity (high vs low) and task (AKs vs FKs) as factors. The main effects of TMS intensity and task were assessed, as well as the interaction between both. In addition, uncorrected pairwise comparisons of the RTs corresponding to the two different TMS intensities were performed separately for each of the motor tasks to exclude even subtle effects of TMS on task performance. Incorrect responses during AKs were discarded during the analysis of RTs. A paired *t* test assessed whether the TMS intensity (TMS_{HIGH} vs TMS_{LOW}) had an impact on the number of incorrect button presses during associative finger tapping.

The functional imaging data were preprocessed and analyzed with FSL4.0 (FMRIB, Oxford University, Oxford, UK). The first two volumes in each experimental run were discarded to allow the brain tissue to reach steady-state magnetization. Preprocessing of the functional time series included motion correction, linear registration to the individual whole-brain EPI (6 degrees of freedom), high-pass filtering (360 s cutoff), and spatial smoothing (Gaussian with 5 mm full-width at half-maximum). The echo time of the EPI readout was selected as short as possible (TE, 20 ms) to minimize image distortions and signal dropout as well as to minimize the BOLD sensitivity of the sequence. Still, because a residual BOLD weighting of the images is still present at this echo time, we decided to explicitly model the BOLD signal in each run as regressor of no interest in addition to the regressors for the perfusion signal (for details, see www.fmrib.ox.ac.uk/fsl/feat5/perfusion.html). This resulted in three regressors (each lasting 9 min 20 s) per run. An alternating intensity variation of constant height between control and tag images was used to model the perfusion baseline and was included in the analysis as regressor of no interest. A block regressor was used to model the alternation between the stimulation and rest periods (20 s OFF at the start of a run followed by three repetitions of 60 s ON–120 s OFF). The regressor of no interest for the residual BOLD activation was modeled as the convolution of this block regressor with a standard hemodynamic response function (HRF). The perfusion activation (i.e., our regressor of interest) was modeled as the multiplication of the regressors for the rCBF baseline and the BOLD signal, thereby implicitly assuming that the stimulus-related perfusion changes have a similar time course as the BOLD signal.

A general linear model (GLM) was estimated separately for each experimental run, and the runs corresponding to the same experimental condition were subsequently combined for each subject in a fixed-effects analysis. At this stage, the analysis of the second session was repeated for two randomly selected subjects to control for putative systematic effects of varying image intensities on the subsequent statistical comparisons across sessions. Generally, the possibility for absolute quantification of rCBF enables robust across-session comparisons in ASL imaging. Here, we use differences in image intensity rather than absolute rCBF values to limit the complexity of the analysis. However, the only parameter of the equation applied for rCBF quantification (Wang et al., 2005a; Moisa et al., 2010) that varied across sessions was the intensity of the control

magnitude images (M_{CON}). Therefore, we obtained two mean M_{CON} images by averaging all control magnitude images separately for each session and scaled the raw functional data of the second session voxelwise by the ratio of the two average M_{CON} images. The results of the GLM analyses were only marginally affected by this scaling, i.e., the effect of global differences in M_{CON} intensities across sessions could be neglected in our study.

To allow for group-level inferences, the maps of the individual parameter estimates (PEs) were normalized to MNI space in a two-step procedure. First, the whole-brain EPI was registered to the individual T1-weighted anatomical image, and then the anatomical image was registered to the MNI template. The normalized individual maps of PEs were fed into a second-level mixed-effects analysis with experimental conditions and subjects as fixed and random factors, respectively. In addition to the covariates of interest, the two different scanning sessions were modeled as additional regressors to further control for unwanted across-session effects. Group *Z*-statistical images were derived using a corrected statistical threshold of $p < 0.05$ at the cluster level based on Gaussian random field theory (Worsley et al., 1996). The threshold for each voxel within a given cluster was set to an uncorrected $p < 0.01$ (corresponding to $Z = 2.3$).

We were specifically interested to elucidate how the TMS-induced perfusion changes depended on the task, as revealed by the interaction between factors TMS and TASK. The corresponding activation map was used to determine five regions of interest (ROIs) for the visualization of the perfusion changes across conditions. The ROIs were first defined based on anatomy and MNI coordinates. The right M1 was defined as the part of the anterior bank of the central sulcus located around the hand knob (Yousry et al., 1997). The right PMd was determined using the junction of the superior precentral sulcus with the superior frontal sulcus. Based on MNI coordinates, an adjacent lateral part of the superior precentral sulcus was determined as the ventral portion of right PMd adjacent to the ventral premotor cortex (PMv) (Tomassini et al., 2007). The area anterior to the ventral PMd ROI was defined as the caudal part of Brodmann area 9 (BA9). The right cingulate motor area (CMA) was determined as the region anterior to the right precentral gyrus and lying within the cingulate sulcus (i.e., inferior to the proper and presupplementary motor areas; Picard and Strick, 2001). The raw ROIs were subsequently intersected with the group activation map for the interaction TMS × TASK. This procedure revealed the ventral portion of right M1, so that an additional control ROI was created for the main part of M1 by intersecting the anatomical ROI with the region showing significant main effects for both tasks versus PV (each thresholded at $z = 6.5$ at the voxel level and then intersected). The ROIs were transformed to the individual low-resolution EPIs. Within each ROI, the statistical PEs were averaged across all voxels. Finally, the PEs were averaged across subjects and plotted for the different conditions.

In addition to standard GLM analysis as outlined above, we used psychophysiological interaction (PPI) analyses (Friston et al., 1997) to investigate how the functional connectivity between the stimulated left PMd and the other motor areas was influenced by the mode of movement selection, TMS intensity, and the interaction between both. The first PPI was used to test for regions showing a change in functional coupling with the left PMd during the associative compared with the free selection task. At the subject level, we first created the input data for the PPI analysis by determining the perfusion subtraction time courses between the control and tagged EPIs for each run. A sinc interpolation was used to create datasets with the same number of volumes as the original input data (for details, see http://www.fmrib.ox.ac.uk/fsl/feat5/perfusion.html). Subsequently, all runs corresponding to either of the two tasks, regardless of TMS intensity, were combined into one dataset. The statistical model contained three main regressors: the physiological and the psychological time series as effects of no interest; multiplication of both revealed the PPI term as the effect of interest. The psychological regressor was obtained by convolving a boxcar waveform coding the contrast of tasks (1 during AKs, −1 during FKs, and 0 during the fixation periods between the task epochs) with a canonical HRF. The physiological regressor was generated by averaging the perfusion time courses across all voxels within a seed region in the targeted left PMd. This region was defined based on the group perfusion activation for factor TMS in the PV condition ($p < 0.01$ at the voxel level; peak coordinates, $x = -20$, $y = -6$, $z = 54$; cluster volume, 128 mm^3). Any putative impact of systematic, but unspecific baseline differences between the runs on the PPI results was ruled out by centering the PMd time courses for each run before building the physiological regressor. The final PPI regressor represented the interaction between the psychological and physiological factors. Seven additional regressors of no interest were used to model the time periods of the first seven runs using boxcar functions, thereby (in combination with the constant term) accounting for any unspecific baseline differences between the eight runs. The subject-specific statistical PPI maps were normalized to MNI space and fed into a second-level mixed-effects analysis to identify consistent changes in functional connectivity at the group level. Using the procedure described above, a second PPI analysis was conducted to compare the associative task with the PV condition. A third PPI analysis was used to test for between-session effects. Here we used the PV periods of both sessions to create the psychological regressor.

Results

None of the participants reported any adverse effects during the course of the experiment. Mean stimulus intensity in the TMS_{HIGH} condition was 62.1 ± 4.7% of maximal stimulator output, whereas mean intensity was 29.5 ± 1.4% of maximal stimulator output for the TMS_{LOW} condition.

Task performance

The behavioral data are summarized in Figure 1. Mean RTs were consistently longer for associative opposed to freely selected responses ($F_{(1,8)} = 137.63$, $p < 0.001$; Fig. 1*C*). This RT difference reflected the different mode of movement selection between the two motor tasks. Subjects were able to decide on the next button press during the interval between two consecutive visual stimuli when they freely selected the key presses. In contrast, no movement preparation was possible in the associative task, resulting in longer RTs. This task-specific difference in RT was not modified by the TMS condition because the interaction between TMS intensity and task was not significant. Accordingly, pairwise comparisons of mean RTs revealed no effect of TMS intensity in both tasks (Fig. 1*E*,*F*). The intensity of TMS had also no effect on mean error rates during AKs (Fig. 1*D*).

Task-related brain activation

Figure 2*A* depicts the brain regions mainly belonging to the frontoparietal core motor network that were consistently activated during both tasks relative to PV, regardless of TMS intensity. Significant rCBF increases were found in the sensorimotor system, including right (contralateral to the site of stimulation) primary sensorimotor area (M1/S1), bilateral cingulate and supplementary motor areas (CMA/SMA), as well as bilateral dorsal and ventral premotor areas (PMv, PMd).

Inspection of the differential task effects for freely selected movements compared with externally instructed movements based on visuomotor associations confirmed primarily matched activity patterns in the frontoparietal core motor network for both tasks. More specifically, at the cluster-corrected level, no brain region within the field of view exhibited significantly stronger rCBF increases during associative relative to free movement selection. The junction between the left supramarginal and angular gyri (peak coordinates, $x = -55$, $y = -52$, $z = 44$; $Z_{peak} = 4.3$; cluster size, 3712 mm^3) was the only area exhibiting increased rCBF for the opposite comparison (freely selected vs associative movements). At a lowered statistical threshold ($Z = 2.3$ at the voxel level, no cluster probability threshold), several areas exhib-

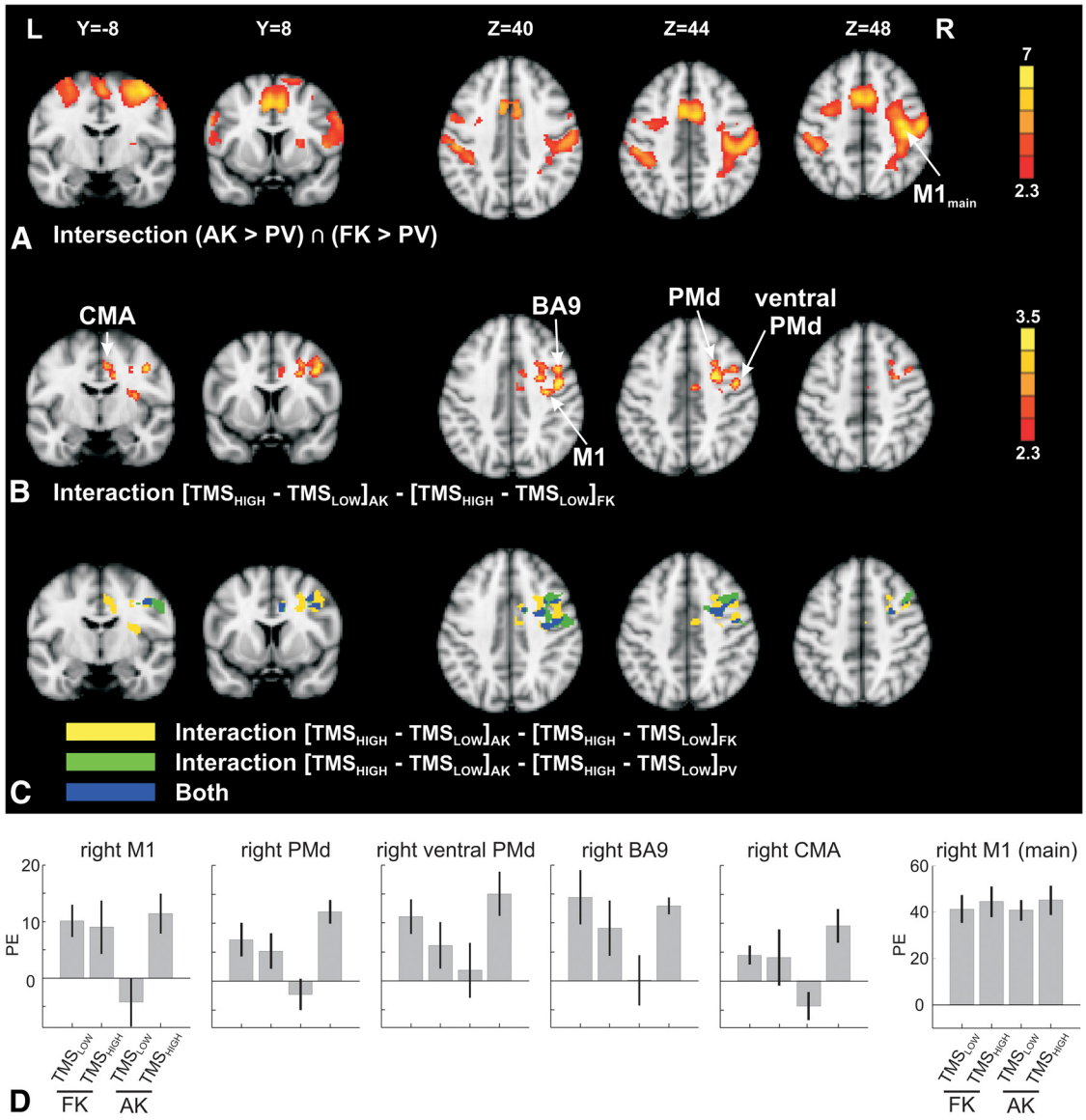

Figure 2. Group rCBF activation maps (MNI space); unless indicated otherwise, a threshold of $Z = 2.3$ (corresponding to $p = 0.01$) at the voxel level and a cluster probability threshold of $p = 0.05$ were used for all figures. ***A***, Regions more strongly activated during both tasks compared with PV. Color coded are the *Z*-values of the comparison AK > PV after masking with the activations for FK > PV. ***B***, Interaction between motor task and TMS intensity $[(TMS_{HIGH} - TMS_{LOW})_{AK} - (TMS_{HIGH} - TMS_{LOW})_{FK}]$. ***C***, Overlap of the results depicted in ***B*** with the interaction between AKs versus PV and TMS intensity $[(TMS_{HIGH} - TMS_{LOW})_{AK} - (TMS_{HIGH} - TMS_{LOW})_{PV}]$. ***D***, To visualize the rCBF changes across conditions, PEs (proportional to the rCBF changes) are shown for six ROIs as indicted by the arrows in ***A*** and ***B***. The error bars represent the SE across subjects.

ited a trend toward increased rCBF during freely selected movements compared with both associative movements and PV (the intersection between the contrasts FK > AK and FK > PV was used to assess "real" rCBF increases during the FK task, thus excluding areas merely showing less deactivation during FK compared with AK). All of these areas were located outside the regions of common task activations shown in Figure 2*A*. The largest clusters were found in the bilateral superior frontal gyri (peak coordinates, $x = 4$, $y = 10$, $z = 63$; $Z_{peak} = 3.0$ for FK > AK; cluster size, 1176 mm^3), the left inferior frontal gyrus (peak coordinates, $x = -38$, $y = 25$, $z = 9$; $Z_{peak} = 2.8$ for FK > AK; cluster size, 408 mm^3), the bilateral medial frontal gyri (peak coordinates, $x = -42$, $y = 37$, $z = 28$; $Z_{peak} = 3.1$ for FK > AK; cluster size, 376 mm^3; and $x = 38$, $y = 34$, $z = 25$; $Z_{peak} = 3.2$ for FK > AK; cluster size, 872 mm^3), and the right supramarginal gyrus (peak coordinates, $x = 49$, $y = -40$, $z = 44$; $Z_{peak} = 3.8$ for FK > AK; cluster size, 2360 mm^3). No regions exhibited the opposite trend, i.e., stronger activations during associative responses compared with both freely selected responses and PV.

Separate analyses of task-related rCBF increases for both tasks revealed comparable peak activations in the targeted left PMd relative to PV (coordinates, $x = -28$, $y = -4$, $z = 54$; $Z_{AK} = 6.6$; $Z_{FK} = 6.7$).

Effect of TMS

The comparison of high versus low TMS intensity revealed significant CBF increases only in one right hemispheric cluster centered on the right inferior parietal lobule and extending into the auditory cortex (peak coordinates, $x = 57$, $y = -41$, $z = 22$; $Z_{peak} = 3.7$; cluster size, 44,144 mm^3). TMS_{HIGH} caused no significant decreases in rCBF relative to TMS_{LOW}. For both motor tasks, interleaved TMS did not have a consistent effect on the rCBF in the left PMd region that was directly stimulated with TMS, even when assessed at a lowered statistical threshold ($Z = 2.3$ at the

Table 1. Interaction associative versus freely selected responses and TMS intensity

Brain region	Coordinates of peak activity			*Z*-value of peak activity	Cluster volume (mm^3)	Cluster volume intersection (mm^3)[a]
	x	*y*	*z*			
Right caudal BA9	42	8	36	3.3	1056	472
Right PMd	26	2	46	3.8	1848	880
Right PMd (ventral part)	44	−6	44	3.7	968	
Right anterior CMA	6	−8	44	3.0	944	512
Right M1	38	−14	38	3.3	512	368
Right insula	34	−10	16	3.1	456	

[a]Intersection volume of the interaction $(TMS_{HIGH} - TMS_{LOW})_{AK} - (TMS_{HIGH} - TMS_{LOW})_{FK}$ with the interaction $(TMS_{HIGH} - TMS_{LOW})_{AK} - (TMS_{HIGH} - TMS_{LOW})_{PV}$ (blue areas in Fig. 2*C*).

voxel level, no cluster threshold). A trend toward an increase in rCBF was observed in left PMd during the PV condition ($Z_{peak} = 2.8$; cluster size, 128 mm^3). This trend increase in rCBF was not located at the hemispheric surface close to the TMS coil but rather deep in the superior frontal sulcus (peak coordinates, $x = -20$, $y = -6$, $z = 54$).

In accordance with our hypothesis, the modulatory effects of TMS on task-related activation depended on the mode of movement selection (Fig. 2*B*; Table 1). Several right hemispheric precentral and mesial cortical motor areas showed a stronger TMS-related increase in rCBF with associative but not with free movement selection, resulting in a significant interaction between TMS intensity and task $[(TMS_{HIGH} - TMS_{LOW})_{AK} - (TMS_{HIGH} - TMS_{LOW})_{FK}]$. These regions included the right M1, the right PMd, the ventral part of the right PMd as well as the adjacent caudal part of right dorsolateral prefrontal cortex, the right anterior insula, and the right anterior CMA. It should be noted that the area designated as right ventral PMd is within the border region to PMv (Tomassini et al., 2007, their Fig. 5) so that its identification remains uncertain to some degree. However, given the tasks under study as well as the TMS coil position (above the left PMd), we suggest it to be more likely a part of PMd.

To graphically illustrate the rCBF changes across conditions, Figure 2*D* shows the PEs (proportional to the rCBF changes) for both motor tasks in six ROIs. The first five ROIs correspond to regions around the main activation peaks revealed by the interaction analysis (Fig. 2*B*). The PE plots reveal that the interaction was predominantly driven by an increase in activation for TMS_{HIGH} versus TMS_{LOW} during associate movements. The sixth ROI served as control ROI and was positioned around the activation peak in right M1 for the main effect of both tasks compared with PV (Fig. 2*A*). The PE plot shows a consistent and robust level of rCBF activation for both tasks and both stimulation intensities. To rule out the impact of unwanted across-session effects on the results presented above, a control analysis tested the interaction between TMS intensity and the PV periods across sessions $[(TMS_{HIGH} - TMS_{LOW})_{PV1} - (TMS_{HIGH} - TMS_{LOW})_{PV2}]$. Visual inspection of the results thresholded at a liberal level of $Z = 1.65$ (equaling $p = 0.05$) uncorrected revealed some spurious activations that overlapped not at all or only by a few negligible voxels with the regions reported above (data not shown). We also tested for brain areas exhibiting TMS-related rCBF increases during AKs compared with PV $[(TMS_{HIGH} - TMS_{LOW})_{AK} - (TMS_{HIGH} - TMS_{LOW})_{PV}]$. Again, right hemispheric precentral and mesial areas showed stronger TMS-related increases in rCBF with associative movement selection relative to the non-motor control task (Fig. 2*C*, green and blue regions). Distinct clusters in the right M1, PMd, BA9, and CMA showed TMS-induced rCBF increases for associative movement selection compared with both free selection and PV (Fig. 2*C*, blue areas; Table 1). TMS had negligible impact on the activity of these areas during PV alone. The contrasts $(TMS_{HIGH} - TMS_{LOW})_{PV}$ and $(TMS_{LOW} - TMS_{HIGH})_{PV}$ did not reveal any signal changes in these regions, even when tested without cluster threshold and at a liberal threshold of $Z = 1.65$ (corresponding to $p = 0.05$) at the voxel level. Thus, the critical effect of TMS can be attributed to a modulation of regional neural activity during the associative task.

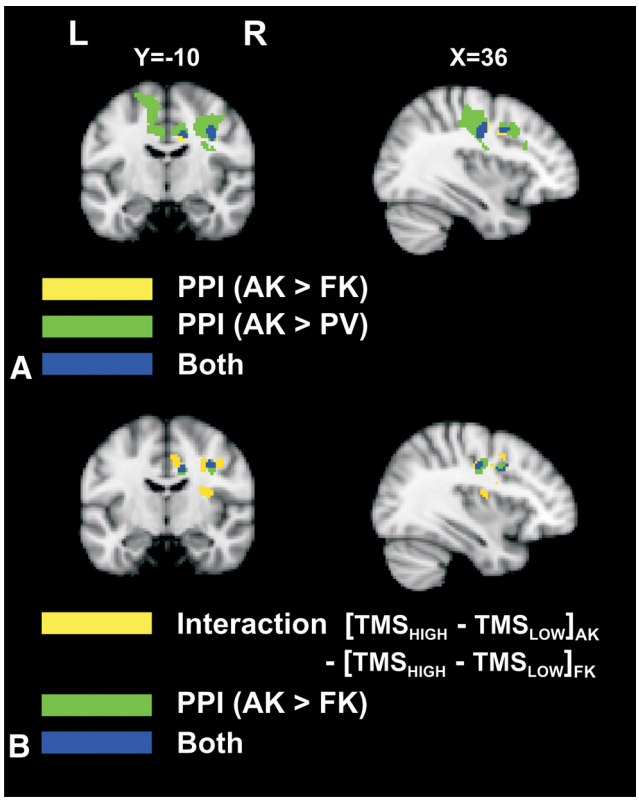

Figure 3. Task-dependent changes in the functional coupling between the left PMd and other motor areas, assessed using PPI analyses. ***A***, Overlap between the PPI results indicating increased coupling for associative versus freely selected movements and the PPI results indicating stronger coupling for associative responses compared with PV. The PPI contrasting associative versus freely selected movements was thresholded at $Z = 1.96$ at the voxel level and a cluster extent threshold of 35 voxels. ***B***, Overlap between the PPI results indicating increased coupling for associative versus freely selected movements and the interaction between AKs versus FKs and TMS intensity (as depicted in Fig. 2*B*).

No TMS-related increases in rCBF were observed during freely selected movements relative to associative movement selection. The regions being sensitive to TMS during associative movement selection mainly showed a consistent task-related activation with free movement selection during both the high- and low-intensity TMS conditions. Similarly, no regions exhibited TMS-related activation increases during free movement selection compared with PV.

The PPI analyses revealed task-dependent changes in functional connectivity between the stimulated left PMd (seed region) and other regions within the motor network. A range of areas (right M1, right PMd, right BA9, left secondary somatosensory motor cortex, bilateral CMA and SMA) showed increased functional coupling for the associative task compared with PV (Fig. 3*A*, blue and green regions). In addition, a second PPI analysis revealed enhanced coupling between the left PMd and a subgroup of these regions (right M1, right BA9, and bilateral CMA) when comparing associative with freely selected responses, using

Table 2. PPI (associative > freely selected responses)

Brain region	Coordinates of peak activity			*Z*-value of peak activity	Cluster volume (mm^3)	Cluster volume intersection (mm^3)[a]
	x	*y*	*z*			
Right caudal BA9	40	2	34	2.4	304	96
Right M1	36	−12	38	2.3	536	408
Bilateral posterior CMA	−10	−26	38	3.1	1024	
	16	−32	40	3.1	1208	

[a]Intersection volume between the PPI results (AK > FK) and the interaction $(TMS_{HIGH} - TMS_{LOW})_{AK} - (TMS_{HIGH} - TMS_{LOW})_{FK}$ (blue areas in Fig. 3*B*).

a more liberal cluster threshold with a minimum *Z*-score of 1.96 ($p = 0.025$) at the voxel level and a cluster extent threshold of 35 voxels (Fig. 3*A*, yellow and blue regions). The areas indentified in this second PPI overlapped with those determined when testing the interaction between TMS intensity and task (Fig. 3*B*, blue regions; Table 2). Finally, the control PPI analysis confirmed that no region within the motor network changed its functional coupling with other brain regions in the field of view when comparing the PV conditions across sessions, even when using a very liberal threshold with an uncorrected $Z = 1.65$ ($p = 0.05$) at the voxel level to minimize the risk for false-negative findings. The similarity between the results of the interaction and PPI analyses supports the view that the direct impact of TMS on the left PMd was driving the remote changes in task-related activity in the right hemispheric areas during the associative task.

Discussion

Our CASL measurements of rCBF revealed that a transient functional perturbation of left PMd induced by online TMS caused an immediate redistribution of neural activity in right-hemispheric premotor and motor areas when healthy volunteers performed visually paced sequential key presses with the left hand. Critically, these increases specifically occurred when movement selection relied on prelearned arbitrary visuomotor associations but not during FKs or PV. In addition, we found context-specific increases in functional coupling between the stimulated left PMd and remote right-hemispheric and mesial motor regions, which were again only present during arbitrary visuomotor mappings.

Importantly, normal task performance was maintained during the application of the rTMS bursts. It is thus safe to conclude that the observed changes in task-related activity and connectivity caused by TMS were not confounded by changes in the behavioral output. Using focal TMS, we tested how the artificial neural activity injected into left PMd spreads along those corticocortical connections that were facilitated by the task under study and impacts on task-related activity in a right-hemispheric functional network during the maintenance and application of arbitrary visuomotor mapping rules. This view is supported by the spatial convergence of the results of the normal GLM analysis and the PPI connectivity analysis.

Using an offline conditioning approach, O'Shea et al. (2007) applied 1 Hz rTMS to left PMd to disrupt the function of left PMd beyond the time of stimulation. This intervention triggered compensatory increases in task-related activity in mesial and right premotor areas for a conditional visuomotor task relative to a control task. Here, we demonstrated immediate rCBF increases during online rTMS in a very similar set of motor cortical areas. This raises the interesting question whether the activity changes in the remote motor cortical areas only reflect context-dependent differences in the spread of excitation along corticocortical connections to these areas. It is conceivable that these remote activity changes might also reflect, at least to some extent, acutely emerging compensatory processes. On the one hand, the observation of TMS-induced activity increases in remote brain areas is consistent with previous findings that even a single TMS pulse can have supra-additive effects on task-related (or stimulus-related) activity at intensities too low to impair behavior (Reichenbach et al., 2011). On the other hand, as in most of previous combined TMS–fMRI studies (Ruff et al., 2006; Bestmann et al., 2008), the "high stimulus intensity" rTMS condition in this study was comparable with online rTMS protocols that have been used to induce "lesion effects" at the behavioral level. It is therefore premature to exclude a compensatory recruitment of additional resources in functionally related remote areas on the basis that TMS did not alter task-related rCBF changes in the left PMd. Although being clearly speculative and beyond the scope of this study, it might be interesting to follow up the question of compensatory processes, in particular of the timescale of their emergence, in future studies.

Externally versus internally guided responses

Our study focused on context-dependent effects of online TMS depending on the mode of movement selection. Both tasks required the preparation and execution of non-stereotyped key-press sequences of similar complexity and activated a frontoparietal core network to a similar extent. Consequently, the task-related differences in the brain response to TMS (as revealed with CASL) cannot be attributed to differences in regional activity in PMd at the time of stimulation. The associative and free movement selections were matched in terms of visual input and motor output, and the timing of the movement was externally cued in both cases. Importantly, the mere presentation of external cues triggered remote activation changes in other premotor regions during stimulation of left PMd only when the external cues guided motor selection based on prelearned visuomotor associations. The mere presentation of the very same cues was not sufficient to trigger such changes when they paced the movement but were irrelevant for action selection. Our study thus helps to resolve the discrepancy on the functional role of PMd between the results of human neuroimaging studies on the one side and electrophysiological recordings in primates and lesion studies in humans and monkeys on the other side. As outlined in the Introduction, neuroimaging studies in humans comparing the contribution of medial and lateral premotor areas with motor control revealed inconsistent results on the specialization of PMd with respect to movement selection (Deiber et al., 1991; Larsson et al., 1996; Jenkins et al., 2000; Weeks et al., 2001), whereas electrophysiological recordings in monkeys demonstrated a gradual dissociation, with PMd neurons being preferentially engaged in mapping external cues onto appropriate responses (Mushiake et al., 1991). Similarly, lesion studies revealed that the loss of PMd resulted in specific behavioral impairments in tasks relying on associative visuomotor mappings (Halsband and Passingham, 1982; Petrides, 1986, 1997; Halsband and Freund, 1990). Our interventional TMS–fMRI approach enabled us to address this controversy by uncovering context-specific connectional fingerprints (Passingham et al., 2004), revealed by a specific TMS-induced shift in activation patterns and providing specific markers of the functional role of the left PMd (Bestmann et al., 2008). The remote effects occurred in a set of areas all contributing to movement selection. This pattern is consistent with the suggested role of the left PMd in coding and predicting learned stimulus–outcome associations, thereby providing this predictive information to a network of other processing nodes in the sensorimotor system (Schubotz, 2007; Grafton et al., 2008). It further suggests that, in addition to the stimulated left PMd, the

uncovered right-hemispheric and mesial motor regions might be key parts of a functional network supporting the maintenance and application of visuomotor mapping.

Combined TMS–fMRI approaches to left PMd function

Our findings significantly extend and strengthen the results of two previous studies combining TMS with fMRI to study the role of left PMd in visuomotor control of hand actions (O'Shea et al., 2007; Bestmann et al., 2008). These studies used PV (Bestmann et al., 2008) or a simple motor execution task (O'Shea et al., 2007) as controls. Our results raise the possibility that their findings were caused by specific TMS effects on the visuomotor mapping performed by the left PMd rather than being attributable to different activation levels between task and control.

As discussed above, O'Shea et al. (2007) demonstrated compensatory activity increases in a similar network of mesial and right premotor areas in response to an offline rTMS intervention for a conditional visuomotor task performed with the right hand. In our case, the TMS-induced shift in the activation pattern occurred during responses with the left hand, consistent with the generalized role of the left PMd in controlling both contralateral and ipsilateral movements (Chen et al., 1997; Schluter et al., 1998; Johansen-Berg et al., 2002; Rushworth et al., 2003).

Using an online perturbation approach, Bestmann et al. (2008) combined event-related TMS with fMRI to target the functional effective connectivity of left PMd. Activity increases in right PMd and M1 during TMS of left PMd occurred only during the visually guided online control of the grip force of the left hand but not at rest. The authors argue that the impact of TMS might depend on the current activation state, resulting in a different interplay between transcallosal inhibition and excitation (Ferbert et al., 1992; Chouinard et al., 2003; Marconi et al., 2003; Mochizuki et al., 2004; Bestmann et al., 2005). We suggest that this explanation likely is too simple, because we observed context-dependent remote effects despite similar activation levels evoked by the two tasks.

Specific remote rCBF responses to TMS were absent in our study during internally guided movements. We hypothesize that the left PMd might be coactivated during this task condition without performing a pivotal functional role. Interestingly, this might partly account for the findings of Siebner et al. (2003) who reported widespread rCBF decreases after 1 Hz rTMS of the left PMd that were similar at rest and during FKs. Consistent with our findings, this indicates that TMS did not result in specific changes of the pattern of movement-related activation during internally guided movements.

Methodological aspects

The subjects responded generally faster when generating freely selected compared with AKs (Fig. 1*C*), because subjects could determine the next response during the time period between two visual cues. When applying prelearned visuomotor mapping rules, participants had to wait for the next cue to be able to select the appropriate response. Importantly, however, the activation levels were comparable in a common parietal–premotor network. In line with previous results (Deiber et al., 1991; Jenkins et al., 2000; Weeks et al., 2001), freely selected responses even tended to engage additional parietal and prefrontal structures compared with both associative responses and PV. This indicates that RT might not be well suited to represent the complexity of the decision processes involved in free selection tasks.

Here we show that the novel approach of interleaving TMS with CASL imaging (Moisa et al., 2010) can be successfully applied to characterize context-dependent effects of TMS on the task-related activation patterns. ASL is insensitive to low-frequency fluctuations and exhibits a reduced inter-subject and inter-session variability compared with BOLD imaging, possibly reflecting a more direct link between rCBF and neural activity (Aguirre et al., 2002; Tjandra et al., 2005; Liu and Brown, 2007). This allowed us to perform random-effects group analyses despite the reduced sensitivity of ASL compared with BOLD fMRI on the single-subject level. The good inter-session reproducibility proved beneficial for comparing the impact of TMS on the two tasks, as confirmed by our several control analyses. Disadvantages of ASL were the limited field of view and the reduced temporal resolution attributable to the alternation between tag and control images. However, ASL offers the possibility to study rCBF changes across longer time periods (Wang et al., 2003, 2005b). This renders ASL imaging particularly suited for assessing the impact of full-fledged repetitive TMS protocols on functional brain connectivity.

Conclusion

The context-dependent effects of left PMd stimulation on motor activity in remote right-hemispheric cortical regions point to a critical involvement of left PMd in mapping external cues on appropriate movements. Effective TMS increased rCBF in these cortical areas only for responses relying on a prelearned associative visuomotor mapping but not for freely selected responses and PV. The data further suggests that the left PMd becomes part of a functional network comprising right-hemispheric and mesial motor regions that supports arbitrary visuomotor mappings with the left nondominant hand. Mapping this acute TMS-induced redistribution of activity with CASL imaging offers important new insights into the causal dynamics of the functional neuroarchitecture of the human brain in health and disease.

References

Aguirre GK, Detre JA, Zarahn E, Alsop DC (2002) Experimental design and the relative sensitivity of BOLD and perfusion fMRI. Neuroimage 15:488–500.

Bédard P, Sanes JN (2009) On a basal ganglia role in learning and rehearsing visual-motor associations. Neuroimage 47:1701–1710.

Bestmann S, Baudewig J, Frahm J (2003) On the synchronization of transcranial magnetic stimulation and functional echo-planar imaging. J Magn Reson Imaging 17:309–316.

Bestmann S, Baudewig J, Siebner HR, Rothwell JC, Frahm J (2005) BOLD MRI responses to repetitive TMS over human dorsal premotor cortex. Neuroimage 28:22–29.

Bestmann S, Swayne O, Blankenburg F, Ruff CC, Haggard P, Weiskopf N, Josephs O, Driver J, Rothwell JC, Ward NS (2008) Dorsal premotor cortex exerts state-dependent causal influences on activity in contralateral primary motor and dorsal premotor cortex. Cereb Cortex 18:1281–1291.

Cavina-Pratesi C, Valyear KF, Culham JC, Köhler S, Obhi SS, Marzi CA, Goodale MA (2006) Dissociating arbitrary stimulus-response mapping from movement planning during preparatory period: evidence from event-related functional magnetic resonance imaging. J Neurosci 26:2704–2713.

Chen R, Cohen LG, Hallett M (1997) Role of the ipsilateral motor cortex in voluntary movement. Can J Neurol Sci 24:284–291.

Chouinard PA, Van Der Werf YD, Leonard G, Paus T (2003) Modulating neural networks with transcranial magnetic stimulation applied over the dorsal premotor and primary motor cortices. J Neurophysiol 90:1071–1083.

Deiber MP, Passingham RE, Colebatch JG, Friston KJ, Nixon PD, Frackowiak RS (1991) Cortical areas and the selection of movement: a study with positron emission tomography. Exp Brain Res 84:393–402.

Eliassen JC, Souza T, Sanes JN (2003) Experience-dependent activation pat-

terns in human brain during visual-motor associative learning. J Neurosci 23:10540–10547.
Ferbert A, Priori A, Rothwell JC, Day BL, Colebatch JG, Marsden CD (1992) Interhemispheric inhibition of the human motor cortex. J Physiol 453:525–546.
Friston KJ, Buechel C, Fink GR, Morris J, Rolls E, Dolan RJ (1997) Psychophysiological and modulatory interactions in neuroimaging. Neuroimage 6:218–229.
Grafton ST, Schmitt P, Van Horn J, Diedrichsen J (2008) Neural substrates of visuomotor learning based on improved feedback control and prediction. Neuroimage 39:1383–1395.
Halsband U, Freund HJ (1990) Premotor cortex and conditional motor learning in man. Brain 113:207–222.
Halsband U, Passingham R (1982) The role of premotor and parietal cortex in the direction of action. Brain Res 240:368–372.
Jankowski J, Scheef L, Hüppe C, Boecker H (2009) Distinct striatal regions for planning and executing novel and automated movement sequences. Neuroimage 44:1369–1379.
Jenkins IH, Jahanshahi M, Jueptner M, Passingham RE, Brooks DJ (2000) Self-initiated versus externally triggered movements. II. The effect of movement predictability on regional cerebral blood flow. Brain 123:1216–1228.
Johansen-Berg H, Rushworth MF, Bogdanovic MD, Kischka U, Wimalaratna S, Matthews PM (2002) The role of ipsilateral premotor cortex in hand movement after stroke. Proc Natl Acad Sci U S A 99:14518–14523.
Larsson J, Gulyás B, Roland PE (1996) Cortical representation of self-paced finger movement. Neuroreport 7:463–468.
Liu TT, Brown GG (2007) Measurement of cerebral perfusion with arterial spin labeling. Part 1. Methods. J Int Neuropsychol Soc 13:517–525.
Marconi B, Genovesio A, Giannetti S, Molinari M, Caminiti R (2003) Callosal connections of dorso-lateral premotor cortex. Eur J Neurosci 18:775–788.
Mochizuki H, Huang YZ, Rothwell JC (2004) Interhemispheric interaction between human dorsal premotor and contralateral primary motor cortex. J Physiol 561:331–338.
Moisa M, Pohmann R, Ewald L, Thielscher A (2009) New coil positioning method for interleaved transcranial magnetic stimulation (TMS)/functional MRI (fMRI) and its validation in a motor cortex study. J Magn Reson Imaging 29:189–197.
Moisa M, Pohmann R, Uludağ K, Thielscher A (2010) Interleaved TMS/CASL: comparison of different rTMS protocols. Neuroimage 49:612–620.
Mushiake H, Inase M, Tanji J (1991) Neuronal activity in the primate premotor, supplementary, and precentral motor cortex during visually guided and internally determined sequential movements. J Neurophysiol 66:705–718.
O'Shea J, Johansen-Berg H, Trief D, Göbel S, Rushworth MF (2007) Functionally specific reorganization in human premotor cortex. Neuron 54:479–490.
Passingham RE, Ramnani N, Rowe JB (2004) The motor system. In: Human brain function, Ed 2 (Frackowiak RSJ, Friston KJ, Frith CD, Dolan RJ, Price CJ, Zeki S, Ashburner J, Penny W, eds), pp 5–32. Amsterdam: Elsevier.
Petrides M (1986) The effect of periarcuate lesions in the monkey on the performance of symmetrically and asymmetrically reinforced visual and auditory go, no-go tasks. J Neurosci 6:2054–2063.
Petrides M (1997) Visuo-motor conditional associative learning after frontal and temporal lesions in the human brain. Neuropsychologia 35:989–997.
Picard N, Strick PL (2001) Imaging the premotor areas. Curr Opin Neurobiol 11:663–672.
Reichenbach A, Whittingstall K, Thielscher A (2011) Effects of transcranial magnetic stimulation on visual evoked potentials in a visual suppression task. Neuroimage 54:1375–1384.
Richter W, Andersen PM, Georgopoulos AP, Kim SG (1997) Sequential activity in human motor areas during a delayed cued finger movement task studied by time-resolved fMRI. Neuroreport 8:1257–1261.
Ruff CC, Blankenburg F, Bjoertomt O, Bestmann S, Freeman E, Haynes JD, Rees G, Josephs O, Deichmann R, Driver J (2006) Concurrent TMS-fMRI and psychophysics reveal frontal influences on human retinotopic visual cortex. Curr Biol 16:1479–1488.
Rushworth MF, Johansen-Berg H, Gobel SM, Devlin JT (2003) The left parietal and premotor cortices: motor attention and selection. Neuroimage 20 [Suppl 1]:S89–S100.
Sakai K, Hikosaka O, Miyauchi S, Sasaki Y, Fujimaki N, Pütz B (1999) Presupplementary motor area activation during sequence learning reflects visuo-motor association. J Neurosci 19:RC1(1–6).
Schluter ND, Rushworth MF, Passingham RE, Mills KR (1998) Temporary interference in human lateral premotor cortex suggests dominance for the selection of movements. A study using transcranial magnetic stimulation. Brain 121:785–799.
Schubotz RI (2007) Prediction of external events with our motor system: towards a new framework. Trends Cogn Sci 11:211–218.
Siebner HR, Filipovic SR, Rowe JB, Cordivari C, Gerschlager W, Rothwell JC, Frackowiak RS, Bhatia KP (2003) Patients with focal arm dystonia have increased sensitivity to slow-frequency repetitive TMS of the dorsal premotor cortex. Brain 126:2710–2725.
Siebner HR, Bergmann TO, Bestmann S, Massimini M, Johansen-Berg H, Mochizuki H, Bohning DE, Boorman ED, Groppa S, Miniussi C, Pascual-Leone A, Huber R, Taylor PC, Ilmoniemi RJ, De Gennaro L, Strafella AP, Kähkönen S, Klöppel S, Frisoni GB, George MS, et al (2009) Consensus paper: combining transcranial stimulation with neuroimaging. Brain Stimul 2:58–80.
Tjandra T, Brooks JC, Figueiredo P, Wise R, Matthews PM, Tracey I (2005) Quantitative assessment of the reproducibility of functional activation measured with BOLD and MR perfusion imaging: implications for clinical trial design. Neuroimage 27:393–401.
Tomassini V, Jbabdi S, Klein JC, Behrens TE, Pozzilli C, Matthews PM, Rushworth MF, Johansen-Berg H (2007) Diffusion-weighted imaging tractography-based parcellation of the human lateral premotor cortex identifies dorsal and ventral subregions with anatomical and functional specializations. J Neurosci 27:10259–10269.
Toni I, Ramnani N, Josephs O, Ashburner J, Passingham RE (2001) Learning arbitrary visuomotor associations: temporal dynamic of brain activity. Neuroimage 14:1048–1057.
Wang J, Aguirre GK, Kimberg DY, Roc AC, Li L, Detre JA (2003) Arterial spin labeling perfusion fMRI with very low task frequency. Magn Reson Med 49:796–802.
Wang J, Zhang Y, Wolf RL, Roc AC, Alsop DC, Detre JA (2005a) Amplitude-modulated continuous arterial spin-labeling 3.0-T perfusion MR imaging with a single coil: feasibility study. Radiology 235:218–228.
Wang J, Rao H, Wetmore GS, Furlan PM, Korczykowski M, Dinges DF, Detre JA (2005b) Perfusion functional MRI reveals cerebral blood flow pattern under psychological stress. Proc Natl Acad Sci U S A 102:17804–17809.
Weeks RA, Honda M, Catalan MJ, Hallett M (2001) Comparison of auditory, somatosensory, and visually instructed and internally generated finger movements: a PET study. Neuroimage 14:219–230.
Worsley KJ, Marrett S, Neelin P, Vandal AC, Friston KJ, Evans AC (1996) A unified statistical approach for determining significant voxels in images of cerebral activation. Hum Brain Mapp 4:58–73.
Yousry TA, Schmid UD, Alkadhi H, Schmidt D, Peraud A, Buettner A, Winkler P (1997) Localization of the motor hand area to a knob on the precentral gyrus: a new landmark. Brain 120:141–157.
Zaharchuk G, Ledden PJ, Kwong KK, Reese TG, Rosen BR, Wald LL (1999) Multislice perfusion and perfusion territory imaging in humans with separate label and image coils. Magn Reson Med 41:1093–1098.
Zhang W, Silva AC, Williams DS, Koretsky AP (1995) NMR measurement of perfusion using arterial spin labeling without saturation of macromolecular spins. Magn Reson Med 33:370–376.